Multi-GNSS Dynamic High Precision Positioning in urban environment

Javier Míguez[1,2], José V. Perello Gisbert[1], J. A. Garcia-Molina[1,3], Paolo Zoccarato[1,4], Paolo Crosta[1], Lionel Ries[1], Raül Orús Pérez[1], Gonzalo Seco-Granados[2], Massimo Crisci[1]

[1]*European Space Agency (ESA)*
[2]*Universitat Autònoma de Barcelona (UAB)*
[3]*HE-Space*
[4]*RHEA*

BIOGRAPHY

Javier Míguez received his M.S. degree in Industrial Systems Engineering, from the Universidad Carlos III de Madrid, Spain, in 2014. He is currently working as a Radio Navigation Engineer at the European Space Agency and employed by Universitat Autònoma de Barcelona. He is working on the performance assessment of Real Time Precise Point Positioning (PPP) for mobile user with Professional (Dual-Frequency) and Mass-Market (Single-Frequency) Receivers using single and multi-GNSS constellations. In addition he is working with performance analysis tools in order to characterize the future GNSS scenario, especially in urban environments but also in rural-open sky.

José V. Perello Gisbert received his M.S. degree in Telecommunications Engineering from the Universidad Politécnica de Valencia, Spain, in 2002. He is currently working in the European Space Agency (ESTEC, the Netherlands) as Galileo Evolutions system performance engineer. Previously he worked for Galileo performance characterization (using GNSS receivers) during In Orbit Validation (IOV), experimentation phase and satellites in orbit testing. He is also managing GNSS R&D activities. Since 2005 he has been supporting the Galileo project.

J.A. Garcia-Molina is a Radio Navigation Engineer at the European Space Agency (Noordwijk, the Netherlands), where he leads several R&D activities on GNSS receiver technology and ground and space applications. His main research interests include signal processing, estimation theory, GNSS receivers and signals, and cloud positioning applications.

Paolo Zoccarato holds a Master in Telecommunication Engineering from University of Padua (Italy) and a PhD in Sciences, Technologies and Measurements for Space from the Centre of Studies and Activities for Space (CISAS) of the University of Padua (Italy) with a PhD thesis on "Precise Orbit Determination (POD) of LEO satellites for Radio Occultation (RO) with GNSS". He worked at Curtin University as a PostDoc on PPP-RTK and in Trimble Terrasat on GNSS network processing for VRS and RTx. Since 2016, he has been a Radio Navigation Engineer consultant for the Radio Navigation Systems & Techniques Section of ESA/ESTEC.

ABSTRACT

Over the last years the carrier based positioning has been receiving more attention as it is used for high accuracy positioning, among the code pseudorange. The main goal of this contribution is to investigate a technique for users in urban environment with the use of GNSS carrier phase measurements for enhancing the accuracy obtained with only code-based techniques.

INTRODUCTION

The use of carrier phase techniques, like the *Precise Point Positioning* (PPP) and *Real Time Kinematic* (RTK), are consolidated approaches for providing precise positioning. This work presents the most relevant results with the use of both techniques from a large test campaign. In this test campaign, the measurements are collected by professional and mass-market GNSS receivers mounted on a vehicle used to drive in urban environments. These data are used to investigate the advantages and drawbacks when using either PPP or RTK techniques with real data. Based on the GNSS observables assessment, algorithm enhancement and some receiver techniques are implemented, they are expected to reduce the performance especially for urban users. Among the mass market receivers, an Android N smartphone have been used to collect raw GNSS measurements, in static conditions to be confident about the truth position. It should be noted that the new Android 7 (Nougat) version brings notable advantages on the location service with the capability to extract the Raw GNSS measurements. This paper shows preliminary code-based and carrier-based positioning results. The use of Doppler Measurements to smooth the raw pseudoranges is also an important achievement in this research.

DUAL-FREQUENCY PPP ALGORITHM

PPP is able to achieve sub-meter precision levels for mobile users in urban environments by using precise positions and clocks with a dual-frequency GNSS receiver. For a good

solution of orbit and clocks, PPP requires a hundred of reference stations globally distributed and it is typically used in post-processing. However, due to the technology development those corrections are nowadays provided by commercial companies and it is expected, in a near future, to be available for all the users.

The PPP algorithm uses as input code and phase observations and precise satellite orbits and clocks, in order to calculate precise receiver coordinates and clock. The standard approach in PPP for handling ionospheric delays is to use a dual-frequency receiver and form the "ionosphere-free" linear combination of L1 and L2 (referring to the first and second frequency) carrier phase and pseudorange observations, that for CDMA measurements equations are:

$$P_{r,i}^{s} = \rho_r^s + dt_r - dt^s + \tau_r^s + \mu_i \iota_r^s + d_{r,i} - d_{,i}^s + \mathrm{M}_{r,i}^s + \varepsilon_{r,i}^s \quad (1)$$

$$\Phi_{r,i}^{s} = \rho_r^s + dt_r - dt^s + \tau_r^s - \mu_i \iota_r^s + \delta_{r,i} - \delta_{,i}^s + \lambda_i w_r^s + \lambda_i M_{r,i}^s + m_{r,i}^s + \epsilon_{r,i}^s \quad (2)$$

Where $P_{r,i}^{s}$ and $\Phi_{r,i}^{s}$ represents respectively the GNSS code and phase measurements between the satellite s and the receiver r at frequency i. Here:

- ρ_r^s is the geometric range.
- dt_r and dt^s are the receiver and satellite clock offsets from GNSS time scale, including the relativistic satellite clock correction.
- τ_r^s is the total slant tropospheric delay (the troposphere is a non-dispersive medium).
- $\mu_i \iota_r^s$ is a frequency-dependent ionospheric delay term, where μ_i is the conversion factor between the signal delay along the ray path on frequency L1, and the signal delay at frequency i.
- $d_{r,i}$ and $d_{,i}^s$ are the receiver and satellite instrumental delays, which are dependent on the code and the frequency i.
- $\delta_{r,i}$ and $\delta_{,i}^s$ are frequency dependent carrier phase instrumental delays.
- $\mathrm{M}_{r,i}^s$ represents the effect of multipath on the code at frequency i.
- $\varepsilon_{r,i}^s$ is the receiver code noise.
- λ_i is the signal wavelength at frequency i.
- w_r^s represents the wind-up effect due to the circular polarization of the electromagnetic signal.
- $M_{r,i}^s = \Phi_{r,i}(0) - \Phi_{,i}^s(0) + N_{r,i}^s$ is the non-integer ambiguity, while $N_{r,i}^s$ is the integer ambiguity, $\Phi_{r,i}(0)$ is the receiver initial phase offset and $\Phi_{,i}^s(0)$ is the satellite initial phase offset.
- $m_{r,i}^s + \epsilon_{r,i}^s$ terms are the carrier phase multipath and noise, respectively.

For GLONASS, that is a FDMA system, the model is a little bit more complicated because of the inter-frequency biases. They can be accounted into the phase and code receiver hardware delays $d_{r,i}^s$ and $\delta_{r,i}^s$, but in this way they become dependent from the satellite too. The code and phase observation models then become

$$P_{r,i}^{s} = \rho_r^s + dt_r - dt^s + \tau_r^s + \mu_i \iota_r^s + d_{r,i}^s - d_{,i}^s + \mathrm{M}_{r,i}^s + \varepsilon_{r,i}^s \quad (3)$$

$$\Phi_{r,i}^{s} = \rho_r^s + dt_r - dt^s + \tau_r^s - \mu_i \iota_r^s + \delta_{r,i}^s - \delta_{,i}^s + \lambda_i w_r^s + \lambda_i M_{r,i}^s + m_{r,i}^s + \epsilon_{r,i}^s \quad (4)$$

The observations coming from all the satellites, corrected for the satellite clock offsets, the dry tropospheric slant delay, are processed together to solve the different unknowns: the receiver coordinates, the non-integer phase ambiguity terms, the receiver clock offset and the wet zenith tropospheric delay. The dual-frequency PPP results for a multi-constellation scenario are based on GPS L1CA/L2P, GLONASS G1/G2, Galileo E1/E5a and BeiDou B1/B2 observables.

With single-frequency PPP, the ionosphere-free linear combination, introduced above, cannot be formed. Mass-market receivers are currently using single-frequency for cost and power consumptions reasons. Since the ionospheric effect will be one of the biggest error sources for such users, the PPP performance results with different ionospheric products will be assessed and compared. The following options are available real-time or with less than 24h latency:

a) *Broadcasted ionospheric corrections* in the navigation message, this method is implemented in real-time.
b) *Rapid Global Ionosphere Map* (GIM) provided by IGS and other organizations, this method can provide better results than case a), but it is limited to 1 or 2 days latency. Therefore it cannot be fully implemented in real-time. In a near future the real-time provision of these products could be envisaged.
c) *Satellite-based Augmentation Systems* (SBAS) corrections, such as the EGNOS, providing ionospheric corrections in real-time.

REAL TIME KINEMATIC

The RTK technique is based on the double-difference (DD) observations and it requires the transmission of the observables of the closest reference station (RS) to the users, along with the position of RS to compute the baseline in between. The transmitted observations must be time tagged in the GNSS time scale and the users must synchronize their observation to those received within 40 microseconds (using their PVT solution is usually sufficient).

RTK approach uses a local dense network of CORS with GNSS receiver, providing high positioning performance in the vicinity of a base station (maximum baseline ~10 or 20km). Differently form the Differential GNSS (DGNSS), RTK uses also the phase observables. The DD cancels out the main errors that drive the stand-alone positioning solution. A differential technique converges much faster

than PPP and achieves performances in the range of few decimeters.

The satellite orbit errors are eliminated by the differentiation, but within certain limits according to the baseline length. The admissible orbit errors in function of the baseline length in order to keep the baseline error within 1 cm are shown in Table 1.

Baseline length (km)	Admissible orbit error (m)
0.1	2500
1.0	250
10	25
100	2.5
1000	0.25

Table 1 Relation between orbit error and corresponding 1 cm baseline error.

This technique is limited to the baseline length, but relaxing the limit in the accuracy (e.g. low-cost receivers) increases the length of the admissible baseline. It can be nowadays exploited in real-time with kinematic users, so it a promising technique for carrier-based positioning in challenging environments.

TOOLS & EQUIPMENT

The following state of the art tools and equipment have been used to perform the study:

1. **Grafnav/Inertial Explorer (IE)** software is a powerful, highly configurable processing engine that allows for the best possible static or kinematic GNSS accuracy using all available GNSS data. It is a Novatel COTS product.
2. **RTKlib** is an open source program package for standard and precise positioning with GNSS. It supports both real-time and post-processing in various positioning modes, special emphasis on Single Point Positioning and Single-Frequency PPP with Android GNSS measurements.
3. **Collection bike**: mobile tests have been conducted by a bike equipped with several GNSS receivers. Data has been collected at the University of Nottingham Ningbo campus in China. The equipment is detailed in the table below:

Product	Type	Model
Antenna		Leica GS10
GNSS Rx	SF MMRx	u-Blox NEO-M8P
GNSS Rx	DF “MM-like” Rx	ComNav K708 OEM
GNSS Rx	DF ProRx	SSN AsteRx2el HDC

Table 2: China Data collection Equipment

4. **Huawei P10:** this Android device 7 version brings notable advantages on the location service. Static tests have been conducted to understand the GNSS Raw measurements and how to use them.

Figure 1: China Data Collection bike

It is worth to highlight the inclusion of ComNav K708 within the equipment for the test campaign. It is considered as an example of the future generation of GNSS Receivers, a low-cost receiver with dual-frequency tracking capability.

DATA SETS AND REFERENCE TRAJECTORY

We have conducted several mobile tests under controlled conditions with the collection bike and smartphone. Table 3 summarizes the description of the analyzed tests:

Data Set	Date	Period	Environment
#1	19/06/2017	30min (loop 1)	Urban
#2	19/06/2017	30min (loop 2)	Urban
#3	20/06/2017	30min (loop 1)	Urban
#4	20/06/2017	30min (loop 2)	Urban
#5	05/07/2017	50min	Rural

Table 3: Description of the PPP/RTK tests

Figure 2: China Route Overview

Figure 3: China Route Street-Level Example

In absence of INS data, the reference trajectory has been performed with the ProRx receiver in a Multi-GNSS differential positioning method in a Forward-Backward processing mode. The ambiguities have been fixed to integer values over 90% of the epochs (see Figure 4).

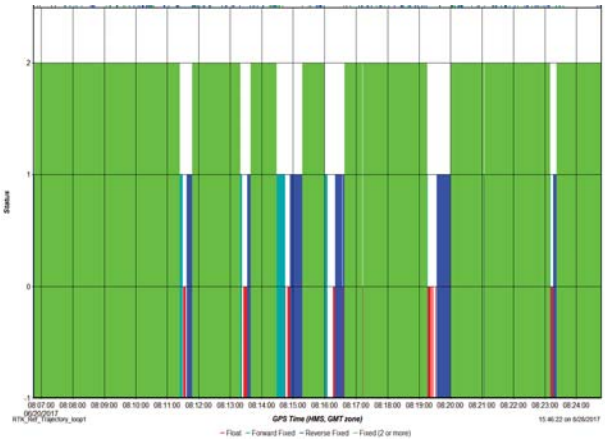

Figure 4: Float/Fixed Ambiguity Status

In previous papers ([**1**][**2**][**3**]), it has been proved that GPS and GLONASS are not enough to give a good carrier-based positioning in terms of availability and accuracy in urban environment. The need of Galileo and BeiDou-3 is a must to achieve sub-meter level accuracy in urban conditions.

The motivation behind the data collection in China is to obtain BeiDou data as third almost complete GNSS constellation after GPS and GLONASS. BeiDou constellation is currently under deployment but it is regionally operational with 5 GEOs and 6 IGSO satellites on top of the MEO satellites. In particular from those IGSO satellites deployed within the regional constellation covering China and neighboring regions. The IGSO satellites can be observed much longer and the corresponding elevation values change much slower than for the MEO satellites. There is a strong correlation between the Signal-to-Noise Ratio (SNR) and Multipath with the elevation. The higher the elevation angles are, the larger the SNR and the smaller the multipath error. Among others, this features makes the IGSO satellites ideal for challenging conditions where the satellite visibility plays a crucial role and the inclusion of the IGSO on top of the already existent GNSS MEO satellites will provide much better geometry and performance.

Galileo and QZSS satellites are also collected in these tests. In overall, a multi-GNSS solution with these real collected data is expected to be at the same level as the solution shown in the previous analyzed studies. This paper tries to validate the results generated synthetically.

OBSERVABLES QUALITY ASSESSMENT

Previously to process the collected data, a detailed assessment of the code and carrier phase measurements has been performed in order to better understand the following results (see from Table 4 to Table 7).

The following figures of merit are considered in the assessment for each of the receivers:

- *Third Order Difference (3^{ord} Diff)*, it is calculated using the following expression:

$$\hat{\varepsilon}^{\varphi}{}_{uncor,c_1}(n) = \frac{\emptyset_{c_1} - 3\emptyset_{c_1}(n-1) + 3\emptyset_{c_1}(n-2) - \emptyset_{c_1}(n-3)}{\sqrt{20}}$$

  where $\emptyset_{c_1}$ is the measured carrier/code phase measurement at epoch n on signal c_1. As the algorithm is time depending, at least four consecutive samples, the signal is separated in different pieces if a loss of signal tracking is found, in order to avoid false spikes.
- *Code-carrier coherence (iono-free) (CCC)*, it is calculated using the following expression:

$$CCC = P_1 - \phi_1 + 2\alpha_1(\phi_2 - \phi_1) - \langle (P_1 - \phi_1 + 2\alpha_1(\phi_2 - \phi_1)) \rangle$$

  This observable combination of code and carrier phase from a dual-frequency receiver is assessed to extract the *multipath error*. It is crucial to detect the cycle-slips correctly beforehand and remove the ambiguity. This Figure of Merit has been computed versus time. In order to shorten the length of the paper and make it more readable only the results from ***Data Set #3*** (see Table 3). Similar results were obtained for the other data sets.

I. SSN AsteRx2 Code/Carrier phase 3^{ord} Diff

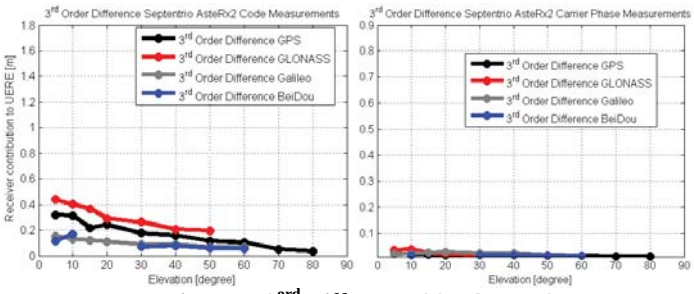

Figure 5: 3^{ord} Difference SSN AsteRx2

II. ComNav K708 Code/Carrier phase 3^{ord} Diff

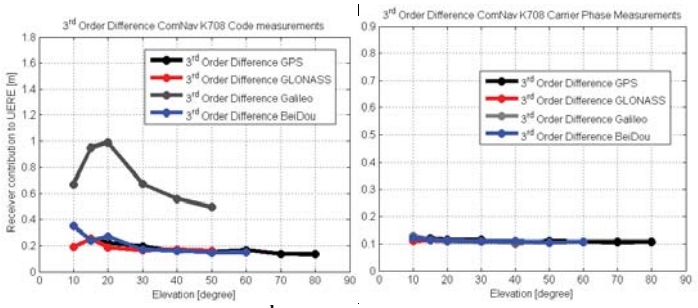

Figure 6: 3^{ord} Difference ComNav K708

III. u-Blox NEO-M8P Code/Carrier phase 3^{ord} Diff

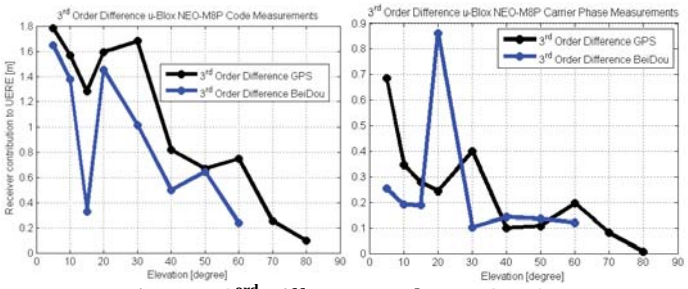

Figure 7: 3^{ord} Difference u-Blox NEO-M8P

The results, as expected, shown a degradation proportionally to the quality, price of the GNSS receiver. *u-Blox NEO-M8P* is a low-cost receiver with, obviously, lower quality clock, oscillator, carrier-phase tracking loop… It is important to remark that all the receivers where connected to the same GNSS antenna. Furthermore, the antenna does not have any impact on this degradation, only the behavior of the receiver plays a role in this comparison.

The receiver contribution is similar among GNSS constellations apart from Galileo in *ComNav K708*. This issue has been further analyzed and outliers satellites were not found. It is then considered a tracking issue for this receiver. However, the outlier found on the tracked BeiDou measurements by u-Blox is clearly due to satellite C06 (see Figure 8). This satellite is affecting considerably the overall receiver contribution and it will be discarded from the analysis at low elevation (<25deg).

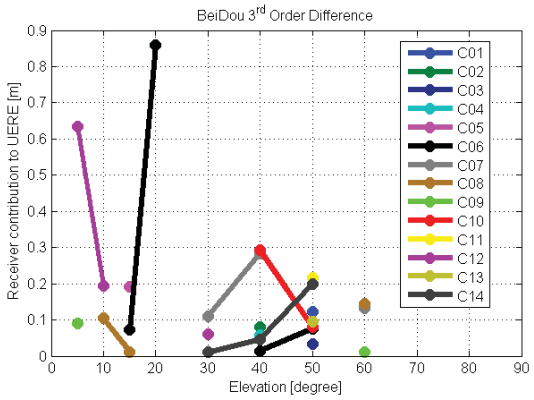

Figure 8: BeiDou 3^{ord} Difference u-Blox NEO-M8P

IV. SSN AsteRx2 and ComNav K708 CCC L1

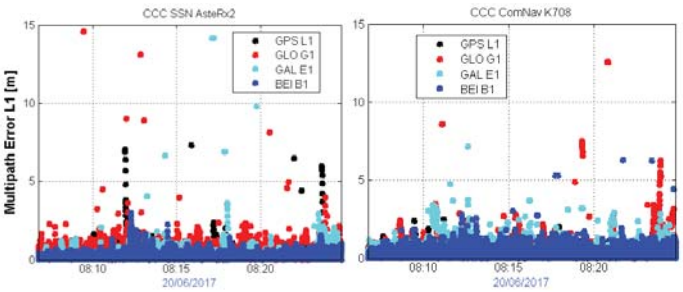

Figure 9: CCC L1 SSN AsteRx2 and ComNav K708

As it can be seen in Figure 9, Similar results have been found for both dual-frequency receivers, multipath slightly higher on *ComNav K708*. GLONASS measurements are more affected from multipath errors and maximum values have been found on same epochs at both receivers.

DYNAMIC SCENARIOS

In the context of dynamic users and urban conditions, the key aspects are the satellite accessibility, multipath and carrier cycle-slips, as the user is moving through the city, it will lose, reacquire and track new satellites continuously, degrading the convergence because the ambiguity has to be solved.

For the generation of these high-accuracy results, Rapid Products are going to be used because nowadays are available with a latency of less than 24 hours (open service) and already provided by commercial services in real-time. It is expected that in a near future the Rapid Products accuracy will be available in real-time for public use. Besides, a professional receiver has been included in the setup for the differential processing. It was located in the surrounding of the data collection (<10km).

I. DF RTK/PPP SSN AsteRx2 Performance.

Data Set #3 PPP Performance	H/V accuracy at 95% [meters]	Positioning Availability
GPS	7.5/13.4	68.13%
GPS+BEI IGSO	9.2/18.9	94.62%
GPS+GLO	8.1/15.1	95.41%
GPS+BEI	2.1/3.3	99.90%
GPS+BEI+GLO	2.1/2.8	99.90%

Table 4: SSN AsteRx2 PPP Performance

Data Set #3 RTK Performance	H/V accuracy at 95% [meters]	Positioning Availability
GPS	0.9/1.3	71.65%
GPS+QZSS	0.9/1.3	73.22%
GPS+QZSS+BEI IGSO	0.6/1.2	77.13%
GPS+GLO	1.0/1.5	90.71%
GPS+BEI	0.2/0.3	99.51%
GPS+BEI+GAL	0.2/0.3	99.61%
GPS+BEI+GAL+GLO	0.6/1.9	93.35%
GPS+BEI+GAL+GLO+QZSS	0.2/0.3	99.61%

Table 5: SSN AsteRx2 RTK Performance

II. DF RTK/PPP ComNav K708.

Data Set #3 PPP Performance	H/V accuracy at 95% [meters]	Positioning Availability
GPS	7.1/10.9	86.71%
GPS+BEI IGSO	2.3/3.6	99.51%
GPS+GLO	5.8/9.0	95.89%
GPS+BEI	1.7/1.9	99.80%
GPS+BEI+GLO	1.7/1.8	99.90%

Table 6: ComNav K708 PPP Performance

Data Set #3 RTK Performance	H/V accuracy at 95% [meters]	Positioning Availability
GPS	1.5/3.8	66.37%
GPS+BEI IGSO	1.5/1.6	81.52%
GPS+GLO	2.0/4.3	84.26%
GPS+BEI	1.1/1.1	97.46%
GPS+BEI+GAL	1.1/1.1	97.46%
GPS+BEI+GAL+GLO	1.3/2.4	88.27%

Table 7: ComNav K708 RTK Performance

III. SF RTK u-Blox NEO-M8P.

Data Set #3 RTK Performance	H/V accuracy at 95% [meters]	Positioning Availability
GPS	1.3/2.7	74.49%
GPS+BEI IGSO	1.1/2.1	82.50%
GPS+BEI	0.7/1.3	96.19%

Table 8: u-Blox NEO-M8P RTK Performance

First of all, Galileo measurements cannot be processed in the PPP algorithm, Grafnav 8.70 is not ready yet to process them. Besides, Single-Frequency PPP is not yet implemented, only single-frequency RTK results will be shown here.

As expected the more GNSS satellites are available the better performance can be achieved. The satellite geometric diversity provided by the multi-GNSS helps to have a greater number of visible satellites and reduce the positioning error. One of the big limitations of PPP is longer convergence times than RTK. The continuous loss of satellites due to the environment (e.g. buildings, trees…) is affecting severely the convergence time, therefore the positioning accuracy. As preliminary conclusions, RTK performs better than PPP in terms of accuracy and gets similar availability in similar conditions, some misleading results will be analyzed in the following sections (see Table 5 and Table 7 highlighted yellow rows). In RTK processing, the GLONASS measurements are degrading the positioning accuracy, most probably because of the IFBs, an expensive receiver calibration has to be done on both station and rover, otherwise they will not totally cancel out in the differentiation.

It is also important to remark the similar results found between *SSN AsteRx2* and *ComNav K708*, although there is a big difference in terms of price between them.

The performance of *RTK u-Blox NEO-M8P* is really good, being at the same order of magnitude as the others two dual-frequency receivers. Again, the performance should not be considered a mass-market representative case because of the professional GNSS antenna used for this data collection.

The impact of IGSO satellites in harsh conditions was of special interest. The inclusion of few IGSO satellites is similar to a full MEO constellation in urban scenarios. (see Table 4 and Table 6). Figure 10 shows that the number of BeiDou IGSO satellites was maximum 3 satellites. However, there were even 8 GLONASS in view.

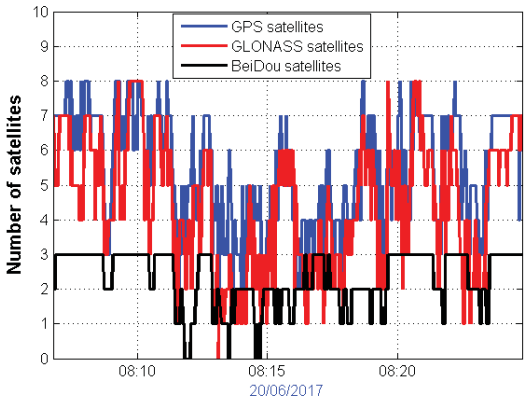

Figure 10: Number of GPS, GLONASS and IGSO BeiDou satellites

Finally, the feasibility of carrier-based positioning in urban environments at sub-meter level is a reality in Asia with the current deployment of BeiDou and Galileo. By 2020, GPS, GLONASS, Galileo and BeiDou will be fully operational, this will involve an increase in the number of visible satellites for PPP/RTK at end user level. Therefore, high accuracy techniques will be able to reach centimeter level positioning accuracy in challenging environments.

Based on the observable quality assessment, together with some receiver techniques are expected to reduce the convergence times and improve the accuracy for urban users. The following improvements will be evaluated:

a) ***Multi-GNSS Elevation Cut-Off Angle***, the quality of the tracked GNSS observables is not the same for all the constellations, each constellation has a different receiver contribution. Based on the 3^{ord} Difference, a different elevation cut-off angle has been defined per constellation:

Receiver	GPS	GLONASS	Galileo	BeiDou
AsteRx2	15deg	15deg	20deg	5deg
ComNav	20deg	15deg	15deg	15deg

Table 9: Settings Multi-GNSS Elevation Cut-Off Angle

b) ***Cycle-Slips Detector***, the carrier cycle slips is one of the key aspects in urban conditions, receiver losses of lock cause discontinuities in the phase measurements that are seen as jumps of integer number of wavelengths. A detector based on the

Melbourne-Wübbena combination is implemented to help the software detect the cycle-slips. This simple algorithm is suitable for running in real time.

The implementation of the following improvements have been applied on the multi-GNSS solutions previously shown (see from Table 4 to Table 7).

SSN AsteRx2	H/V accuracy at 95% [meters]	Positioning Availability
RTK Performance		
GPS+BEI+GAL	0.2/0.3	99.61%
GPS+BEI+GAL+GLO	0.6/1.9	93.35%
GPS+BEI+GAL+GLO+QZSS	0.2/0.3	99.61%
RTK Performance (Elevation + CS Filtering)		
GPS+BEI+GAL+GLO	0.2/0.3	99.61%
PPP Performance		
PPP GPS+BEI+GLO	2.1/2.8	99.90%
PPP Performance (Elevation + CS Filtering)		
PPP GPS+BEI+GLO	0.7/0.6	99.90%

Table 10: AsteRx2 Performance. Algorithm Improvements

ComNav K708	H/V accuracy at 95% [meters]	Positioning Availability
RTK Performance		
GPS+BEI+GAL	1.1/1.1	97.46%
GPS+BEI+GAL+GLO	1.3/2.4	88.27%
RTK Performance (Elevation + CS Filtering)		
GPS+BEI+GAL+GLO	0.3/0.5	99.51%
PPP Performance		
PPP GPS+BEI+GLO	1.7/1.9	99.90%
PPP Performance (Elevation + CS Filtering)		
PPP GPS+BEI+GLO	0.8/0.5	99.90%

Table 11: ComNav Performance. Algorithm Improvements

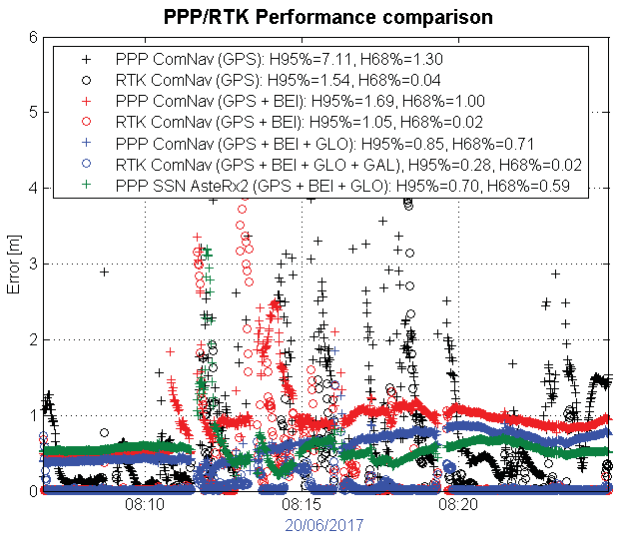

Figure 11: PPP/RTK ComNav Performance Comparison

In summary with a good selection of satellites and a good cycle-slip detector to remove those phase discontinuities that leads to false ambiguities resolution, the performance of PPP/RTK techniques is at sub-meter level in urban conditions.

As it can be seen in Figure 12, RTK converges instantaneously to centimeter level. It is also important to remark that multi-GNSS PPP solution also converges in few epochs but at decimeter level, there is a noise floor due to the dynamic of the user and the receiver contribution from the observables (see Figure 6), not being able to achieve below that. A GPS-only PPP solution needs a couple of minutes to reach the same positioning accuracy and the poor satellite geometry due to the urban environment is driven the accuracy.

As expected, the increase of number of satellites in view, helps considerably to remove gaps, outliers and get a smoother solution.

STATIC SCENARIO

This chapter describes the positioning capabilities available with the new Android devices to understand how far they are from other commercial low-cost receivers.

In order to better understand the performance and have a reliable reference position, a static data collection in rural conditions have been considered as benchmark. It should be highlighted that the system is not providing the pseudorange straightforward, some GNSS engineering is needed to obtain them and the GNSS time. [6]

The different user applications can access to the GNSS data using the framework API location (see Figure 12).

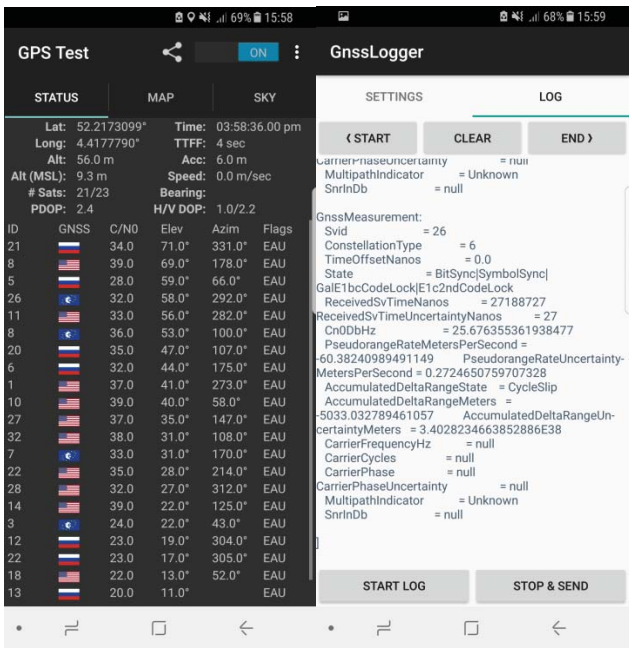

Figure 12: Android GNSS data: GPSTest.apk (left) and GNSSlogger.apk (right)

The following scenario consists of live signal data recorded in ESTEC, The Netherlands. The main assumptions are listed below:

I. Multi-GNSS measurements (GPS, GLONASS and Galileo). 4 Galileo satellites were correctly tracked by the device.

II. Reference Position: It has been computed by RTKLib with Combined Static SF PPP Forward-Backward processing.

III. Techniques:
- Code-based Weighted Least Squares (WLS).
- Single-Frequency PPP.
- Single-Frequency RTK.

IV. Additional products:
- MGEX Orbit/Clock Final Products.
- SBAS ionospheric corrections.

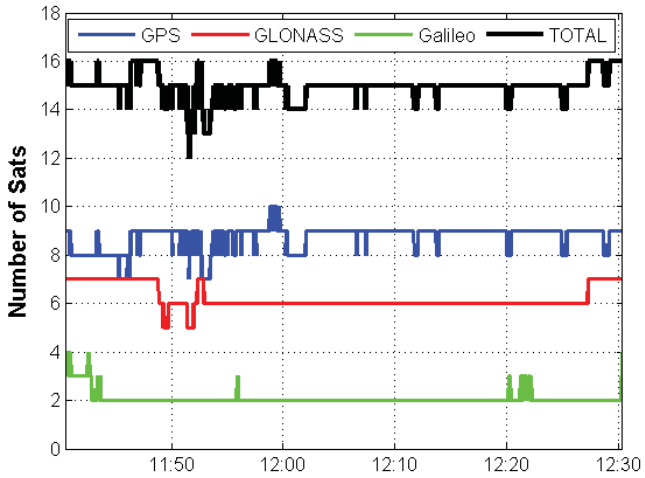

Figure 13: Android GNSS Number of Satellites. Data Set #5

Android GNSS Rural Performance	H/V accuracy at 95% [meters]	Positioning Availability
PVT GPS	16.1/34.6	97.42%
PVT GPS + GAL	15.5/33.7	99.60%
PVT GPS + GAL + GLO	16.4/32.8	99.73%
SF PPP GPS (static algorithms)	1.92/1.68	99.70%
SF PPP GPS + GAL	1.60/1.65	99.75%
SF RTK GPS	8.85/17.5	99.90%
SF RTK GPS + GAL	8.87/15.9	100.00%

Table 12: Android N GNSS PVT/PPP/RTK Performance

In Table 12, it can be seen that the Galileo increases the positioning availability and accuracy. However, GLONASS Raw data might degrade the accuracy but increase the availability. Besides, GLONASS carrier phases, so-called in android Accumulated Delta Range Meters (ADR), are ignored by RTKLib. The Doppler measurements provided by android can be used to smooth raw pseudoranges in difficult environments [7]. The sampling window used to smooth the pseudoranges also plays an important role, several time windows have been compared in order to find the most convenient:

- Doppler Smoothing 5sec.
- Doppler Smoothing 10sec.
- Doppler Smoothing 20sec.
- Doppler Smoothing 100sec.

Doppler Smoothing Assessment	H/V/3D accuracy at 95% [meters]	Positioning Availability
PVT GPS + GAL + GLO	16.4/16.9/35.4	99.73%
PVT GPS + GAL + GLO (5sec)	8.5/17.6/18.4	99.63%
PVT GPS + GAL + GLO (10sec)	7.2/14.5/15.3	99.73%
PVT GPS + GAL + GLO (20sec)	7.3/12.0/13.3	99.63%
PVT GPS + GAL + GLO (100sec)	17.9/34.4/38.5	99/63%

Table 13: Android N GNSS PVT/PPP/RTK Performance

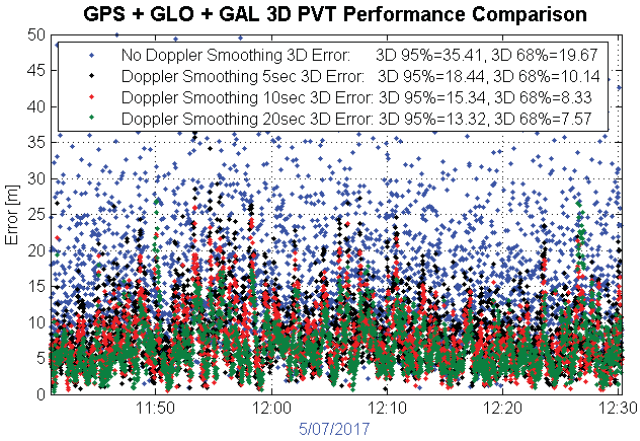

Figure 14: Doppler Smoothing PVT Comparison. Data Set #5

The previous figures show a considerable improvement when using the Doppler measurements to smooth the raw pseudoranges. In future data collections, it will be interested to investigate if the Doppler measurements are also helping in dynamic users. Doppler data might not follow accurately the dynamic of the user.

CONCLUSION

The main goal of this contribution was to characterize the current positioning algorithms in urban environments with the use of GNSS carrier phase measurements (processed with PPP and RTK) with real collected data. This also will validate the characterization performance from the previous studies. Furthermore, improvements for the current algorithms have been proposed and their performance enhancement demonstrated. Finally, the understanding of the positioning capabilities and performance of the new android N version have been presented.

In Asia, BeiDou-2 is regionally operational with the deployment of GEO, IGSO and MEO satellites covering China. In urban environment, the performance of IGSO satellites is similar to a full MEO constellation. This paper shows that with the current deployment of Galileo and BeiDou, together with a good selection of satellites and

cycle-slip detection, carrier-based positioning (in the form of PPP and RTK) can achieve decimeter precision level in harsh-urban conditions. The high number of satellites (more than 80) and the geometry diversity from all the different constellations helps to have a great number of satellites in view continuously, reducing data gaps and outliers.

Another important conclusion is the performance of single-frequency RTK with u-Blox M8P, proving that high accuracy positioning with mass-market receivers can achieve sub-meter level in a near future. This technology improvement on mass-market receivers will do carrier-based positioning interesting to a broad range of applications.

Besides, the android N devices have notable advantages on the location services which might bring plenty of new users to the high accuracy positioning field. But it is still far from achieving high accuracy positioning. Some aspects have to be further analyzed and improved:

- Accumulated Delta Range (ADR) measurements are not as accurate as the common carrier phase measurements from commercial receivers.
- The low quality of the smartphone antenna and ADR makes impossible for RTK techniques to fix ambiguities.

Both PPP and RTK techniques are demonstrated to be feasible in challenging conditions. RTK performs better and is already available in real-time, but the main RTK limitation is the need of a reference station tracking the same GNSS constellations as the rover in the vicinity (distance lower than 10-20km). The advantage of PPP is that it does not need any reference station and the continuous algorithm development will make orbits and clock products available also real-time for all users.

REFERENCES

[1] Míguez, J., Perello-Gisbert, José V., Orus-Perez, R., Garcia-Molina, J., Multi-GNSS PPP performance assessment with different ranging accuracies in challenging scenarios. ION GNSS+ 2016.

[2] Míguez, J., Perello-Gisbert, José V., Orus-Perez, R., Garcia-Molina, J., Real-time multi-GNSS PPP kinematic performance assessment in challenging scenarios. NAVITEC 2016.

[3] Míguez, J., Perello-Gisbert, José V., Orus-Perez, R., Garcia-Molina, J., System Volume Simulation for Carrier Phase Positioning. NAVITEC 2016.

[4] Kaplan, E. and Hegarty, C., *Understanding GPS: Principles and Applications, 2nd Edition, Artech House, Boston, 2005.*

[5] J. Sanz Subirana, J.M. Juan Zornoza and M. Hernández-Pajares, *GNSS Data Processing, Volume I: Fundamentals and Algorithms.* ESA TM-23/1. ISBN 978-92-9221-886-7. European Space Agency. May 2013.

[6] Diggelen, Frank van. "*Android Raw Measurements Tutorial: GNSS clock, Masurements & Navigation Data*", ION GNSS+ 2016.

[7] Bahrami, Mojtaba, and Marek Ziebart. "*Instantaneous Doppler-aided RTK positioning with single frequency receivers*." Position Location and Navigation Symposium (PLANS), 2010 IEEE/ION. IEEE, 2010.

[8] Humphreys, Todd E., et al. "*On the feasibility of cm-accurate positioning via a smartphone's antenna and GNSS chip.*" Position, Location and Navigation Symposium (PLANS), 2016 IEEE/ION. IEEE, 2016.

[9] Cai, Changsheng, et al. "C*ycle slip detection and repair for undifferenced GPS observations under high ionospheric activity.*" GPS solutions 17.2 (2013): 247-260.

[10] Kim, Euiho, Todd Walter, and J. D. Powell. "*Adaptive carrier smoothing using code and carrier divergence.*" Proc. ION NTM. 2007.

[11] Niell, A., 1996. *Global Mapping Functions for the Atmosphere Delay at Radio Wavelengths. Journal of Geophysical Research.*

[12] Miguel M. Romay, María D. Laínez, *Generation of Precise Orbit and Clock Products for A-GNSS.*

[13] Sébastien Carcanague, *Low-cost GPS/GLONASS Precise Positioning Algorithm in Constrained Environment.*

[14] Geng JH, Bock Y, *Triple-frequency GPS precise point positioning with rapid ambiguity resolution.*

[15] Taro Suzuki, Nobuaki Kubo, Tomoji Takasu, *Evaluation of Precise Point Positioning Using MADOCA-LEX via Quasi-Zenith Satellite System.*

[16] Thomas Grinter, Craig Roberts, *Real Time Precise Point Positioning: Are we there yet?*

[17] Pedro Silva, *Cycle Slip Detection and Correction for Precise Point Positioning.*